Nonlinear Optics (WiSe 2018/19)
Lecture 5: November 16, 2018

4.9 Optical parametric amplification (OPA)

4.10 Optical parametric oscillation (OPO)

Chapter 5: The electro-optic effect and modulators

5.1 The linear electro-optic effect

5.1.1 Longitudinal electro-optic effect and modulators

5.1.2 Transverse electro-optic effect and modulator

5.2 Electro-optic amplitude modulator

5.3 Electro-optic phase modulator

5.4 Microwave modulator

4.9 Optical parametric amplification (OPA)

Already for difference-frequency generation it became obvious, that in this frequency mixing process, gain can be achieved. We inspect this process now more generally taking into account losses and without the assumption of perfect phase matching. This will allow us to derive the underlying equations governing the amplification process, its gain bandwidth and associated amplifier noise. We keep the assumption of a constant pump wave at ω_3. Then it holds

symmetric in 1 and 2

$$\frac{\partial \hat{E}(\omega_1)}{\partial z} + \alpha_1 \hat{E}(\omega_1) = -j\kappa_1 \hat{E}(\omega_3) \hat{E}^*(\omega_2) e^{j\Delta kz} \tag{4.115}$$

$$\frac{\partial \hat{E}(\omega_2)}{\partial z} + \alpha_2 \hat{E}(\omega_2) = -j\kappa_2 \hat{E}(\omega_3) \hat{E}^*(\omega_1) e^{j\Delta kz}. \tag{4.116}$$

We again look for an exponential solution $\hat{E}(\omega_1) \sim \hat{E}_0(\omega_1) e^{\gamma' z + j\Delta kz/2}$, and $\hat{E}(\omega_2) \sim \hat{E}_0(\omega_2) e^{\gamma' z + j\Delta kz/2}$, with suitable initial values denoted by the index 0. It follows

$$\left\{ \gamma' + \alpha_1 + \frac{j\Delta k}{2} \right\} \hat{E}_0(\omega_1) + \left\{ j\kappa_1 \hat{E}(\omega_3) \right\} \hat{E}_0^*(\omega_2) = 0 \tag{4.117}$$

$$-\left\{ j\kappa_2 \hat{E}^*(\omega_3) \right\} \hat{E}_0(\omega_1) + \left\{ \gamma' + \alpha_2 - \frac{j\Delta k}{2} \right\} \hat{E}_0^*(\omega_2) = 0. \tag{4.118}$$

From the determinant condition, it follows

$$\gamma'^2 + \gamma'\{\alpha_1 + \alpha_2\} + \alpha_1\alpha_2 + (\Delta k/2)^2 + (\alpha_2 - \alpha_1)\frac{j\Delta k}{2} - \kappa_1\kappa_2\left|\hat{E}(\omega_3)\right|^2 = 0$$

$$\Rightarrow \gamma' = -\frac{(\alpha_1 + \alpha_2)}{2} \pm \left\{\left[\frac{\alpha_1 - \alpha_2}{2} + \frac{j\Delta k}{2}\right]^2 + \kappa_1\kappa_2\left|\hat{E}(\omega_3)\right|^2\right\}^{1/2} \qquad (4.119)$$

For the case of phase matching and no losses, we find

$$\gamma^2 = \kappa_1\kappa_2\left|\hat{E}(\omega_3)\right|^2 \qquad (4.120)$$

For the case of equal losses $\alpha_1 = \alpha_2 = \alpha$, we obtain

$$\gamma' = -\alpha \pm \left\{\gamma^2 - (\Delta k/2)^2\right\}^{1/2} = -\alpha \pm g, \qquad (4.121)$$

where

$$g = \left\{\gamma^2 - (\Delta k/2)^2\right\}^{1/2}. \qquad (4.122)$$

The solutions of the coupled equations (4.115)-(4.116) are of the form

$$\hat{E}(\omega_1, \ell) = e^{-\alpha\ell + j(\Delta k/2)\ell}\left\{\hat{E}_0(\omega_1)\cosh g\ell + B\sinh g\ell\right\} \qquad (4.123)$$

$$\hat{E}(\omega_2, \ell) = e^{-\alpha\ell - j(\Delta k/2)\ell}\left\{\hat{E}_0(\omega_2)\cosh g\ell + D\sinh g\ell\right\} \qquad (4.124)$$

Insertion into the coupled equations (4.115)-(4.116) yields

$$B = -j\frac{\Delta k}{2g}\hat{E}_0\left(\omega_1\right) - j\frac{\kappa_1}{g}\hat{E}\left(\omega_3\right)\hat{E}_0^*\left(\omega_2\right) \qquad (4.125)$$

$$D = -j\frac{\Delta k}{2g}\hat{E}_0\left(\omega_2\right) - j\frac{\kappa_2}{g}\hat{E}\left(\omega_3\right)\hat{E}_0^*\left(\omega_1\right). \qquad (4.126)$$

Note the symmetry between both solutions. Anyway, the two waves are generally called signal and idler wave. If the optical parametric amplifier (OPA) is seeded by one wave only and if $\omega_1 \neq \omega_2$, then this wave is amplified independent of the phase

$\sinh^2 = \cosh^2 - 1$

$$\left|\frac{\hat{E}\left(\omega_1,\ell\right)e^{\alpha\ell}}{\hat{E}_0\left(\omega_1\right)}\right|^2 = \left\{\cosh^2 g\ell + \left(\Delta k/2g\right)^2\sinh^2 g\ell\right\} = \frac{1}{g^2}\left\{\gamma^2\cosh^2 g\ell - \left(\Delta k/2\right)^2\right\}$$

$$(4.127)$$

We define the parametric gain as

$$G_1\left(\ell\right) = \left|\frac{\hat{E}\left(\omega_1,\ell\right)e^{\alpha\ell}}{E_0\left(\omega_1\right)}\right|^2 - 1 \Rightarrow G_1\left(\ell\right) = \left(\gamma\ell\right)^2\frac{\sinh^2 gl}{\left(g\ell\right)^2} \qquad (4.128)$$

Note that for small gain, i.e., $\gamma < \Delta k$, the gain has the form

g becomes imaginary:
$\sinh \rightarrow \sin$

$$G_1\left(\ell\right) = \left(\gamma\ell\right)^2\frac{\sin^2\left\{\left[\left(\Delta k/2\right)^2 - \gamma^2\right]^{1/2}\ell\right\}}{\ell^2\left\{\left(\Delta k/2\right)^2 - \gamma^2\right\}}, \qquad (4.129)$$

that can me further simplified to

$$G_1\ (\ell) = (\gamma\ell)^2 \frac{\sin^2(\Delta k\ell/2)}{(\Delta k\ell/2)^2}$$

for $\gamma \ll \Delta k/2$. In the opposite limit for large gain $\gamma \gg \Delta k/2$

$$G_1\ (\ell) = (\gamma\ell)^2 \frac{\sinh^2 g\ell}{(g\ell)^2} \Rightarrow \frac{1}{4} e^{2g\ell}. \tag{4.130}$$

We define the bandwidth of the OPA via

$$\{(\Delta k/2)^2 - \gamma^2\}^{1/2} \ell = \pi, \tag{4.131}$$

that for small gain implies $\Delta k = 2\pi/\ell$, as we already found for frequency doubling. In general, we obtain from Eq. (4.131)

$$\frac{2\pi\Delta f}{c} = \Delta k = \left\{1 + \left(\frac{\gamma\ell}{\pi}\right)^2\right\}^{1/2} (2\pi/\ell). \tag{4.132}$$

This means that the bandwidth increases with the gain. For the ratio between the bandwidths at high and low gain, we obtain

$$\frac{\Delta f_{\text{High Gain}}}{\Delta f_{\text{Low Gain}}} = \{1 + (\gamma\ell/\pi)^2\}^{1/2}. \tag{4.133}$$

Fig. 4.15 shows the gain as function of $\Delta k\ell$ for various values of $\gamma\ell$.

gain bandwidth increases with stronger pumping

noncollinear type-I OPAs feature ultrabroad bandwidth for few-optical-cycle pulse generation ($\rightarrow$ later lecture)
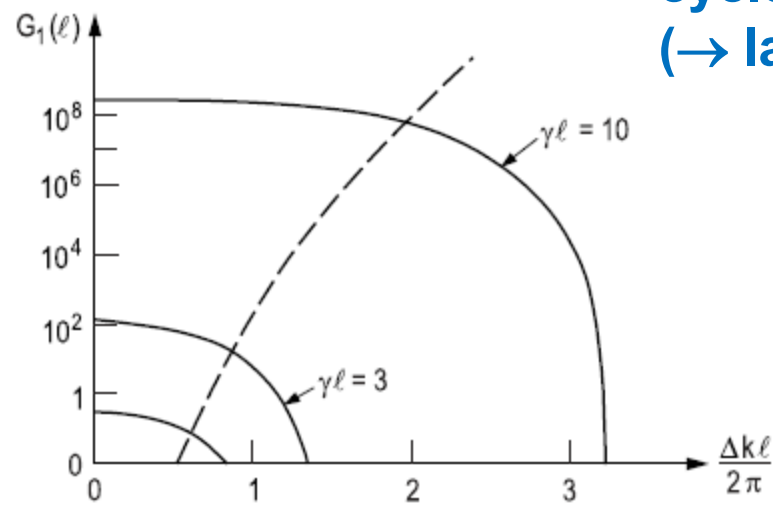

Figure 4.15: Gain of an optical parametric amplifier (OPA) as function of the wave number difference and gain.

4.10 Optical parametric oscillation (OPO)

In a single pass through a parametric amplifier medium, which is described by Eqs. (4.123)-(4.126), the signal and idler waves grow when phase-matched ($\Delta k = 0$) according to

$$\hat{E}(\omega_1, \ell) e^{\alpha_1 \ell} = \hat{E}_0(\omega_1) \cosh \gamma\ell - j\frac{\kappa_1}{\gamma} \hat{E}(\omega_3) \hat{E}_0^*(\omega_2) \sinh \gamma\ell \qquad (4.134)$$

$$\hat{E}(\omega_2, \ell) e^{\alpha_2 \ell} = \hat{E}_0(\omega_2) \cosh \gamma\ell - j\frac{\kappa_2}{\gamma} \hat{E}(\omega_3) \hat{E}_0^*(\omega_1) \sinh \gamma\ell. \qquad (4.135)$$

Most often parametric amplifiers only permit gain for passage in a single direction. In the other direction, only damping occurs

$$\hat{E}'(\omega_1, \ell) = \hat{E}_0(\omega_1) e^{-\alpha_1 \ell}$$

$$\hat{E}'(\omega_2, \ell) = \hat{E}_0(\omega_2) e^{-\alpha_2 \ell}$$

If feedback of the parametric amplifier is realized by means of a Fabry-Pérot resonator and if the field is larger after a round trip than at the beginning, so the amplifier is turned into a self-starting oscillator. The threshold condition is that the losses must equal the gain

$$\hat{E}_0'(\omega_1) = \hat{E}_0(\omega_1)$$

$$\hat{E}_0'(\omega_2) = \hat{E}_0(\omega_2)$$

or inserted into Eqs. (4.134)-(4.135) it follows with $e^{-2\alpha\ell} \sim 1 - 2\alpha\ell$

$$\frac{\hat{E}_0(\omega_1)}{1 - 2\alpha_1 \ell} = \hat{E}_0(\omega_1) \cosh \gamma\ell - j\frac{\kappa_1}{\gamma}\hat{E}(\omega_3)\hat{E}_0^*(\omega_2)\sinh\gamma\ell$$

$$\frac{\hat{E}_0^*(\omega_2)}{1 - 2\alpha_2 \ell} = \hat{E}_0^*(\omega_2) \cosh \gamma\ell + j\frac{\kappa_2}{\gamma}\hat{E}^*(\omega_3)\hat{E}_0(\omega_1)\sinh\gamma\ell.$$

Again the solution of this equation system is only non-zero, if the determinant of the coefficient matrix vanishes, i.e.,

$$\left[\cosh\gamma\ell - \frac{1}{1 - 2\alpha_1\ell}\right]\left[\cosh\gamma\ell - \frac{1}{1 - 2\alpha_2\ell}\right] = \frac{\kappa_1\kappa_2}{\gamma^2}\left|\hat{E}(\omega_3)\right|^2\sinh^2\gamma\ell = \sinh^2\gamma\ell$$

so that

$$1 - \cosh\gamma\ell\left(\frac{1}{1 - 2\alpha_1\ell} + \frac{1}{1 - 2\alpha_2\ell}\right) + \left(\frac{1}{1 - 2\alpha_2\ell}\right)\left(\frac{1}{1 - 2\alpha_1\ell}\right) = 0 \quad (4.136)$$

or

$$\cosh\gamma\ell = 1 + \frac{2\alpha_1\alpha_2\ell^2}{1 - \alpha_1\ell - \alpha_2\ell}. \quad (4.137)$$

For $\alpha_1 \approx \alpha_2 \approx \alpha$ and the case of small losses or small gain $\alpha\ell, \gamma\ell \ll 1$, it follows

$$(\gamma\ell)^2 \approx 4\alpha\ell. \qquad \cosh x = 1 + \frac{x^2}{2!} \quad (4.138)$$

One distinguishes between doubly resonant parametric oscillators (DROs) and singly resonant ones (SRO). In the first case, both signal and idler waves are resonant, in the second case only the signal wave. The threshold for SROs is many times higher than for DRO. Nevertheless, most OPOs are singly resonant, because it is much more difficult to operate a DRO.

8

In an arbitrary coordinate system we can express the index ellipsoid (sometimes also called optical indicatrix) or the inverse dielectric susceptibility tensor as quadratic form

$\rightarrow$ Boyd

$(1/n^2)_i$ connected to dielectric permeability tensor ε_{ij}

$$\left(\frac{1}{n^2}\right)_1 x^2 + \left(\frac{1}{n^2}\right)_2 y^2 + \left(\frac{1}{n^2}\right)_3 z^2 + 2\left(\frac{1}{n^2}\right)_4 yz + 2\left(\frac{1}{n^2}\right)_5 xz + 2\left(\frac{1}{n^2}\right)_6 xy = 1,$$

$$(5.1)$$

introducing the contracted notation using 1-6. If the coordinate system coincides with the principle-axis system of the index ellipsoid, the mixed terms vanish. For the case of the linear electro-optic effect, an applied electric field leads to a deformation of the index ellipsoid according to

$$\Delta\left(\frac{1}{n^2}\right)_i = \sum_{j=1}^{3} r_{ij} E_j,$$

$$(5.2)$$

with $E_1 = E_x$, $E_2 = E_y$, $E_3 = E_z$. It thus follows, e.g.,

$$\Delta\left(\frac{1}{n^2}\right)_1 = r_{11} E_x + r_{12} E_y + r_{13} E_z,$$

$$(5.3)$$

or

$$\begin{pmatrix} \Delta(1/n^2)_1 \\ \Delta(1/n^2)_2 \\ \Delta(1/n^2)_3 \\ \Delta(1/n^2)_4 \\ \Delta(1/n^2)_5 \\ \Delta(1/n^2)_6 \end{pmatrix} = \begin{pmatrix} r_{11} & r_{12} & r_{13} \\ r_{21} & r_{22} & r_{23} \\ r_{31} & r_{32} & r_{33} \\ r_{41} & r_{42} & r_{43} \\ r_{51} & r_{52} & r_{53} \\ r_{61} & r_{62} & r_{63} \end{pmatrix} \begin{pmatrix} E_x \\ E_y \\ E_z \end{pmatrix}.$$

$$(5.4)$$

The coefficients r_{ij} are typically of the order 1 pm/V. The form of the r-matrix depends, as the second-order susceptibility or piezoelectric tensor, on crystal symmetry. The polarization as a result of mechanical forces can be described by

$$
\begin{pmatrix} P_x \\ P_y \\ P_z \end{pmatrix} = \begin{pmatrix} d_{11} & d_{12} & d_{13} & d_{14} & d_{15} & d_{16} \\ d_{21} & d_{22} & d_{23} & d_{24} & d_{25} & d_{26} \\ d_{31} & d_{32} & d_{33} & d_{34} & d_{35} & d_{36} \end{pmatrix} \begin{pmatrix} \sigma_{11} \\ \sigma_{22} \\ \sigma_{33} \\ \sigma_{23} \\ \sigma_{13} \\ \sigma_{13} \\ \sigma_{12} \end{pmatrix} .
$$

Here the σ_{ij} are the tensile, compressional, and shear stress, and the coefficients d_{ij} represent the piezoelectric tensor. Table 5.1 provides examples of the electro-optic coefficients of the 7 crystal systems.

Table 9.1. *The electro-optic $\overline{\overline{r}}$ for the 32 crystal symmetry classes.* · *zero element,* • *nonzero element,* •——• *equal nonzero elements,* •------o *equal nonzero elements of opposite sign. Centrosymmetric classes – all elements of $\overline{\overline{r}}$ are zero.*

Triclinic

$$\begin{pmatrix} \bullet & \bullet & \bullet \\ \bullet & \bullet & \bullet \\ \bullet & \bullet & \bullet \\ \bullet & \bullet & \bullet \\ \bullet & \bullet & \bullet \\ \bullet & \bullet & \bullet \end{pmatrix}$$

Example: Calcium thiosulphate ($CaS_2O_3.6H_2O$) strontium tartrate ($SrH_2(C_4H_4O_6)_2.4H_2O$)

Monoclinic

$$\begin{pmatrix} \cdot & \bullet & \cdot \\ \bullet & \cdot & \cdot \\ \cdot & \bullet & \cdot \\ \bullet & \cdot & \bullet \\ \cdot & \bullet & \cdot \\ \cdot & \bullet & \bullet \end{pmatrix}$$

2 (symmetry axis parallel to y)

$$\begin{pmatrix} \cdot & \cdot & \bullet \\ \cdot & \cdot & \bullet \\ \cdot & \cdot & \bullet \\ \bullet & \bullet & \cdot \\ \bullet & \bullet & \cdot \\ \cdot & \cdot & \bullet \end{pmatrix}$$

2 (symmetry axis parallel to z)

Examples: lithium sulphate ($LiSO_4.H_2O$), tartaric acid triglycine sulphate

$$\begin{pmatrix} \bullet & \cdot & \bullet \\ \bullet & \cdot & \bullet \\ \bullet & \cdot & \bullet \\ \cdot & \bullet & \cdot \\ \cdot & \bullet & \cdot \\ \bullet & \cdot & \bullet \end{pmatrix}$$

m (perpendicular to y)

$$\begin{pmatrix} \bullet & \bullet & \cdot \\ \bullet & \bullet & \cdot \\ \bullet & \bullet & \cdot \\ \cdot & \cdot & \bullet \\ \cdot & \cdot & \bullet \\ \bullet & \bullet & \cdot \end{pmatrix}$$

m (perpendicular to z)

Example: potassium nitrite (KNO_2)

Orthorhombic

$$\begin{pmatrix} \cdot & \cdot & \cdot \\ \cdot & \cdot & \cdot \\ \cdot & \cdot & \cdot \\ \bullet & \cdot & \cdot \\ \cdot & \bullet & \cdot \\ \cdot & \cdot & \bullet \end{pmatrix}$$

222

Examples: α–iodic acid (α–HIO_3), magnesium sulphate ($MgSO_4.7H_2O$), Rochelle salt ($KNaC_4H_4O_6.4H_2O$)

$$\begin{pmatrix} \cdot & \cdot & \bullet \\ \cdot & \cdot & \bullet \\ \cdot & \cdot & \bullet \\ \cdot & \bullet & \cdot \\ \bullet & \cdot & \cdot \\ \cdot & \cdot & \cdot \end{pmatrix}$$

mm2

Examples: Barium sodium niobate ($Ba_2NaNb_5O_{15}$), polyvinylidine fluoride (PVF), $(CH_2CF_2)_n$

11

Table 9.1. (cont.)

Tetragonal
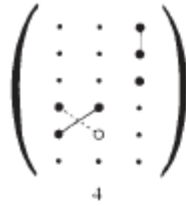
Example: iodo succinimide $(CH_2CO)_2NI$

4
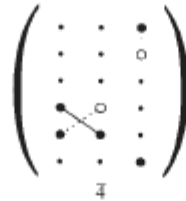
Examples: pentaerythritol $(C(CH_2OH)_4)$, cahnite $(Ca_4B_2As_2O_{12}.4H_2O)$

$\bar{4}$
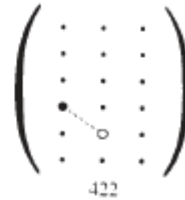
Example: nickel sulphate $NiSO_4.6H_2O$

422

Example: $BaTiO_3$

4 mm
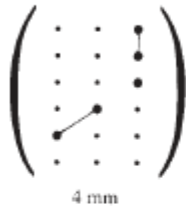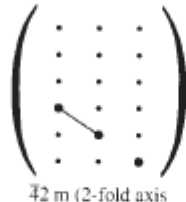
Examples: KDP, ADP, $CdGeAs_2$, $AgGaSe_2$, $AgGaS_2$

$\bar{4}2$ m (2-fold axis parallel to x)

Cubic
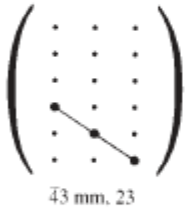
Examples: $(\bar{4}3$ m): GaAs, InAs, GaP, ZnSe, CdTe, InSb, (23): Sodium chlorate $(NaClO_3)$, sodium bromate $(NaBrO_3)$

$\bar{4}3$ mm, 23
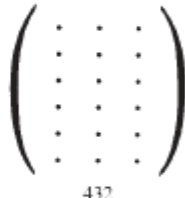
432 (lacks a center of symmetry, but other symmetry elements make all elements zero)

Trigonal

Example: sodium periodate $NaIO_4.3H_2O$

Examples: quartz, Te, mercury sulphide $(\alpha-HgS)$

3m (m perpendicular to x) standard orientation
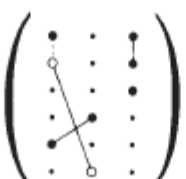
Examples: $LiNbO_3$, $LiTaO_3$, proustite (Ag_3AsS_3), pyragyrite (Ag_3SbS_3)

3m (m perpendicular to y)

$LiNbO_3$ is <u>THE</u> crystal for EOMs

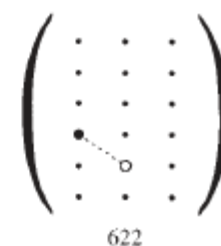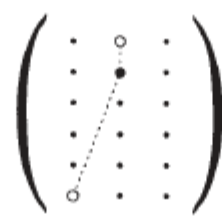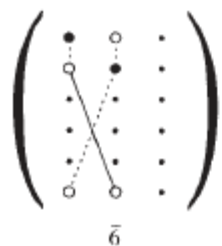Table 9.1. (*cont.*)

Hexagonal

6
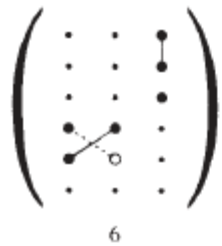
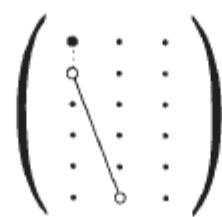Examples:
lithium iodate
(LiIO$_3$),
Iodoform (CHI$_3$)

6 mm

Examples:
CdS, CdSe,
ZnS, ZnO

622

Examples:
barium
aluminate
(BaAl$_2$O$_4$)
kalsilite
(KAlSiO$_4$)

$\bar{6}$

$\bar{6}$ m2 (m perpendicular to x)
standard orientation

Examples:
benitoite (BaTiSi$_3$O$_9$)

$\bar{6}$ m2 (m perpendicular to y)

13

For an applied field, the index ellipsoid changes according to

$$\left[\frac{1}{n_1^2} + \Delta\left(\frac{1}{n^2}\right)_1\right] x^2 + \left[\frac{1}{n_2^2} + \Delta\left(\frac{1}{n^2}\right)_2\right] y^2 + \left[\frac{1}{n_3^2} + \Delta\left(\frac{1}{n^2}\right)_3\right] z^2$$
$$+2\left[\frac{1}{n_4^2} + \Delta\left(\frac{1}{n^2}\right)_4\right] yz + 2\left[\frac{1}{n_5^2} + \Delta\left(\frac{1}{n^2}\right)_5\right] xz + 2\left[\frac{1}{n_6^2} + \Delta\left(\frac{1}{n^2}\right)_6\right] xy = 1,$$

$$(5.5)$$

If the crystal is oriented along the principle axes, it follows

$$\left[\frac{1}{n_1^2} + \Delta\left(\frac{1}{n^2}\right)_1\right] x^2 + \left[\frac{1}{n_2^2} + \Delta\left(\frac{1}{n^2}\right)_2\right] y^2 + \left[\frac{1}{n_3^2} + \Delta\left(\frac{1}{n^2}\right)_3\right] z^2$$
$$+2\Delta\left(\frac{1}{n^2}\right)_4 yz + 2\Delta\left(\frac{1}{n^2}\right)_5 xz + \Delta\left(\frac{1}{n^2}\right)_6 xy = 1.$$

$$(5.6)$$

It becomes immediately clear, that the linear electro-optic effect can only occur in non-centrosymmetric media, otherwise it would require

$$\Delta\left(\frac{1}{n^2}\right)_i = \sum_{j=1}^{3} r_{ij} E_j = -\sum_{j=1}^{3} r_{ij} E_j,$$

$$(5.7)$$

i.e., all coefficients would vanish. In general, changes in the index ellipsoid can

electric field generates also stress in a crystal due to the inverse piezo-electric effect. For low frequencies, the crystal displacements can follow the stress due to the electric field. For high frequencies that is not necessarily the case and therefore one has to expect that the coefficients for this process are different for low and high frequencies

$$r_{ij}^{dc} \neq r_{ij}^{hf}.$$

For an isotropic medium with photo-elastic effect, we have

$$\frac{1}{n^2} - \frac{1}{n_0^2} = pS, \tag{5.8}$$

or in short

$$\Delta n = \frac{n_0^3}{2} pS, \tag{5.9}$$

where p is the photo-elastic or elasto-optic coefficient, and S is the deformation. Eq. (5.9) is for example useful to describe the index change due to an acoustic wave. In the anisotropic case, the photo-elastic effect is described by

$$\Delta \left(\frac{1}{n^2} \right)_i = \sum_{k=1}^{6} \pi_{ik} \sigma_k, \tag{5.10}$$

where π_{ik} denotes the elasto-optic coefficients and σ_k the stress values.

5.1.1 Longitudinal electro-optic effect and modulators

To see how the electro-optic effect is used for the construction of modulators, we consider the case of potassium dihydrogen phosphate (KDP, KH_2PO_4). The related materials (KD*P, KD_2PO_4), ammonium dihydrogen phosphate (ADP, $(NH_4)(H_2PO_4)$) or (AD*P, $(NH_4)(D_2PO_4)$) behave similarly. These materials belong to the crystal class $\overline{4}2m$ and the electro-optic tensor has the form

$$
\mathbf{r} = \begin{pmatrix} 0 & 0 & 0 \\ 0 & 0 & 0 \\ 0 & 0 & 0 \\ r_{41} & 0 & 0 \\ 0 & r_{41} & 0 \\ 0 & 0 & r_{63} \end{pmatrix}. \tag{5.11}
$$

If we apply an electric field $\mathbf{E} = E_x\mathbf{e}_x + E_y\mathbf{e}_y + E_z\mathbf{e}_z$, we obtain for the index ellipsoid

$$
\frac{x^2 + y^2}{n_0^2} + \frac{z^2}{n_e^2} + 2r_{41}E_x yz + 2r_{41}E_y xz + 2r_{63}E_z xy = 1. \tag{5.12}
$$

If we have a field with only a z-component

$$\frac{x^2 + y^2}{n_0^2} + \frac{z^2}{n_e^2} + 2r_{63}E_z xy = 1. \tag{5.13}$$

Since the equation is symmetric in x and y, the main axes are rotated by 45° against the x-y-coordinate system and z is invariant (see Fig. 5.1)

$$x = x' \cos 45° + y' \sin 45°, \tag{5.14}$$
$$y = -x' \sin 45° + y' \cos 45°. \tag{5.15}$$
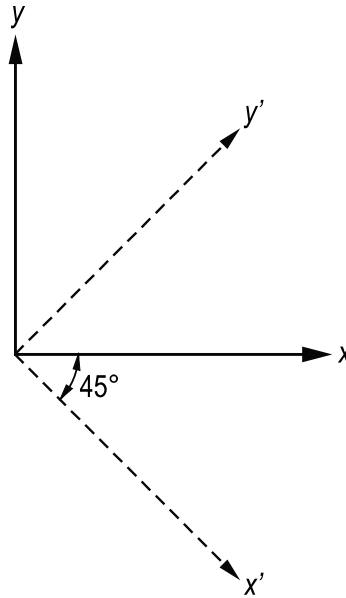
Figure 5.1: Rotation of the main axes for the $\overline{4}2$m symmetry class for the case of an electric field applied in z-direction.

Substitution into Eq. (5.13) leads to

$$\left(\frac{1}{n_0^2} - r_{63}E_z\right) x'^2 + \left(\frac{1}{n_0^2} + r_{63}E_z\right) y'^2 + \frac{z^2}{n_e^2} = 1. \qquad (5.16)$$

Due to the applied field, the crystal becomes slightly biaxial and shows along the main axes the refractive indices

$$n_{x'}^2 = \frac{n_0^2}{1 - n_0^2 r_{63}E_z}; \quad n_{y'}^2 = \frac{n_0^2}{1 + n_0^2 r_{63}E_z}; \quad n_{z'}^2 = n_e^2. \qquad (5.17)$$

Since the changes in refractive index are small, i.e., $n_0^2 r_{63}E_z \ll 1$,

$$n_{x'} = n_0 \left(1 + \frac{1}{2} n_0^2 r_{63}E_z\right); \; n_{y'} = n_0 \left(1 - \frac{1}{2} n_0^2 r_{63}E_z\right); \quad n_{z'} = n_e. \qquad (5.18)$$

If a wave propagates inside the crystal in z-direction, the different polarizations experience a phase shift with respect to each other

$$\Delta\phi = \frac{2\pi L}{\lambda_0}\left(n'_x - n'_y\right) = \frac{2\pi L n_0^3 r_{63} E_z}{\lambda_0}. \tag{5.19}$$

The crystal thus acts as a voltage-dependent waveplate. The half-wave voltage, i.e., the voltage for a differential phase shift of π, is

$$V_\pi = \frac{\lambda_0}{2n_0^3 r_{63}}. \tag{5.20}$$

For KDP with $r_{63} = -10.5$ pm/V, $n_0 = 1.51$ at a wavelength of 632.8 nm, the half-wave voltage is $V_\pi = 8752$ V. If the input wave is rotated by 45° with respect to the x', y' axes, see Fig. 5.2, i.e., parallel to the x or y axis, then the half-wave plate turns the polarization by 90°. If the voltage is continuously increased to V_π, then the polarization evolves from initially linear to circular and finally again linear polarization, see Fig. 5.3. The polarization evolution can be used to construct a modulator.
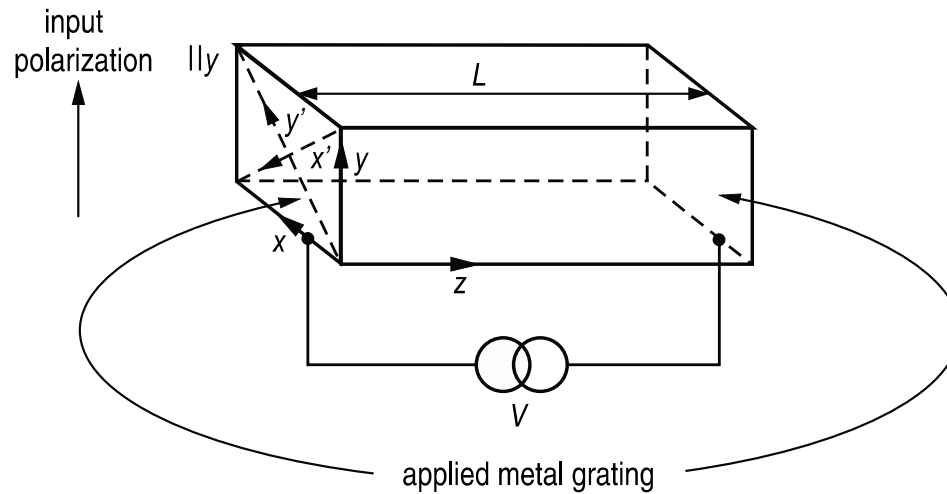
Needs electrodes on input and output facets

Figure 5.2: KDP crystal orientation for a longitudinal electro-optic modulator.

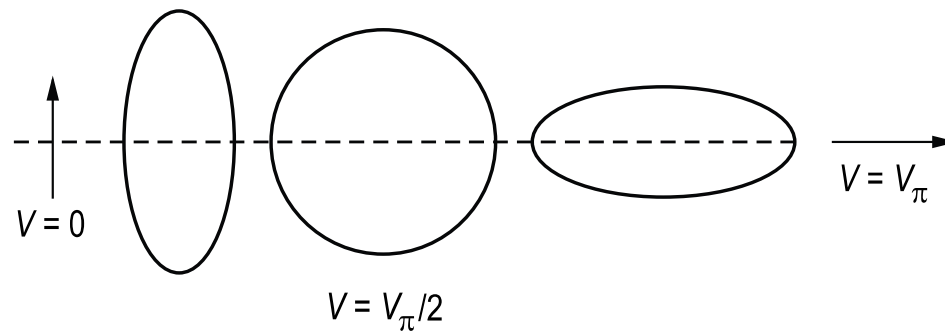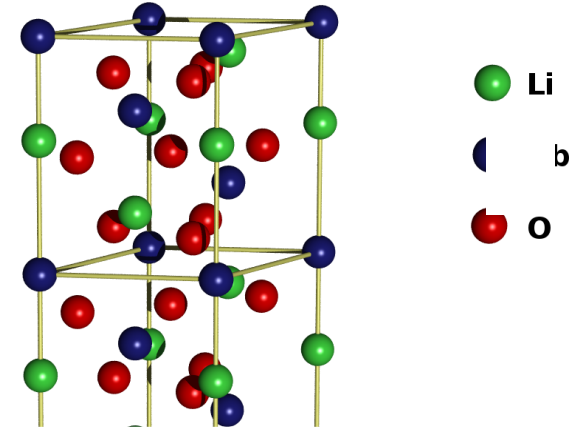
Figure 5.3: Change in polarization state along propagation through the crystal due to the electro-optic phase retardation as shown in Fig. 5.2.

lithium niobate:

LiNbO$_3$

crystal class 3m

$$\mathbf{r} = \begin{pmatrix} 0 & -r_{22} & r_{13} \\ 0 & r_{22} & r_{13} \\ 0 & 0 & r_{33} \\ 0 & r_{51} & 0 \\ r_{51} & 0 & 0 \\ -r_{22} & 0 & 0 \end{pmatrix} \cdot$$

Li

b

O

The index ellipsoid for the crystal without applied voltage has the form

$$\frac{x^2}{n_0^2} + \frac{y^2}{n_0^2} + \frac{z^2}{n_e^2} = 1. \tag{5.22}$$

With a field applied in y-direction, the index ellipsoid reads

$$\left(\frac{1}{n_0^2} - r_{22}E_y \right) x^2 + \left[\left(\frac{1}{n_0^2} + r_{22}E_y \right) y^2 + \frac{z^2}{n_e^2} + 2r_{51}E_y yz \right] = 1. \tag{5.23}$$
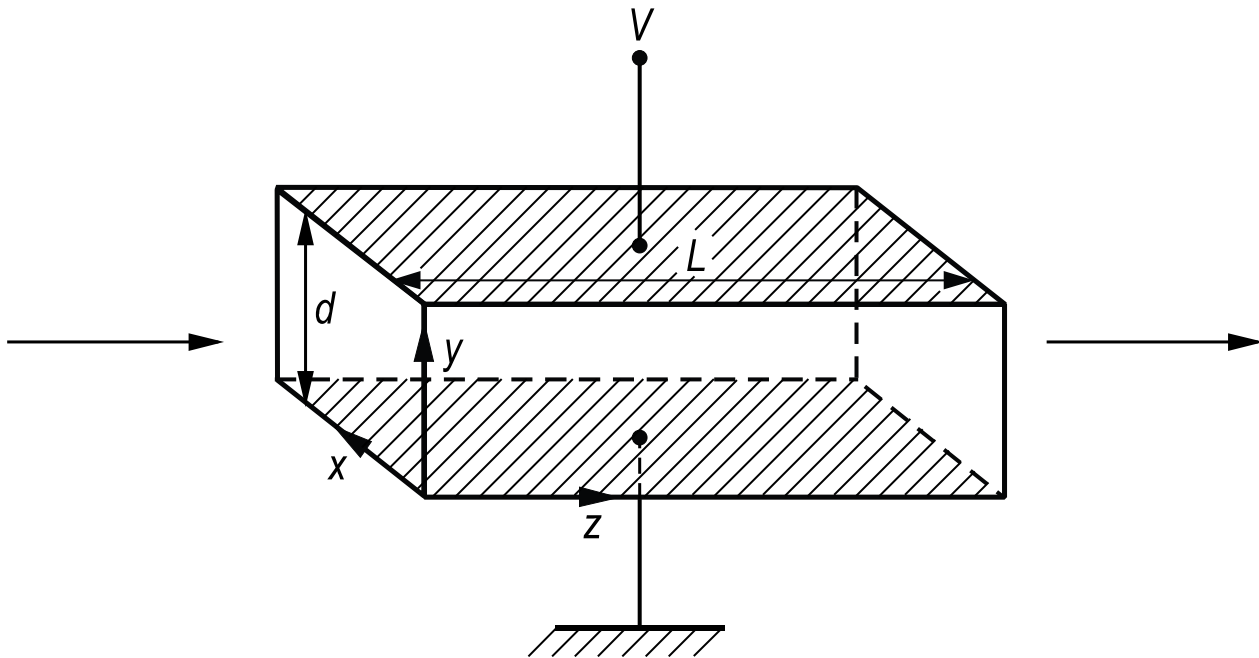
Figure 5.4: Orientation of a LiNbO$_3$ crystal to implement a transverse electro-optic modulator.
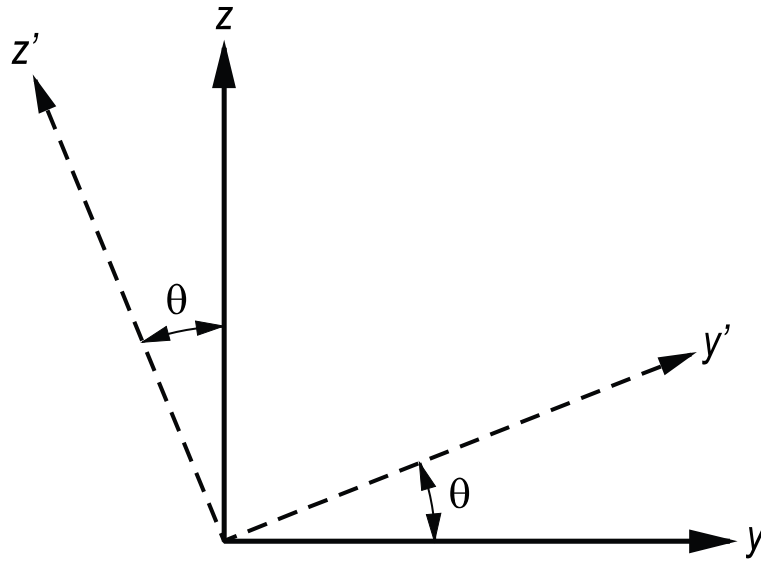
Figure 5.5: Rotation of the main axes in LiNbO$_3$, if an electric field is applied along the y-axis.

Because of the cross-term yz, the main axes are not preserved, and we transform to a new system, see Fig. 5.5, via

$$
\begin{aligned}
x &= x' \\
y &= y' \cos\theta - z' \sin\theta \\
z &= z' \cos\theta + y' \sin\theta.
\end{aligned}
\tag{5.24}
$$

The x-axis remains invariant and stays a main axis. Substitution into Eq. (5.23) leads to the following condition, that the cross-term vanishes

$$\left(\frac{1}{n_e^2} - \frac{1}{n_0^2} - r_{22}E_y\right) \sin\theta \cos\theta + r_{51}E_y(2\cos^2\theta - 1) = 0. \qquad (5.25)$$

Typically, the nonlinear coefficients are small and therefore also the necessary angle of rotation θ is small, i.e., $\theta \sim \sin\theta$ and $\cos\theta \sim 1$, and therefore θ simplifies to

$$\theta = \frac{-r_{51}E_y}{(1/n_e^2 - 1/n_0^2 - r_{22}E_y)}. \qquad (5.26)$$

With the corresponding values for lithium niobate, $r_{51} = 28 \cdot 10^{-12}$m/V, $r_{22} = 3.4 \cdot 10^{-12}$m/V, $n_e = 2.21$, $n_0 = 2.3$ and an applied voltage of 1 kV across a 1-mm-thick crystal, we obtain

$$\theta = \frac{-28 \times 10^{-12} \times 10^6}{\left(\frac{1}{2.21}\right)^2 - \left(\frac{1}{2.3}\right)^2 - 3.4 \times 10^{-12} \times 10^6} = 1.78 \text{ mrad } = 0.1°.$$

Thus, the angle θ is really small. Since LiNbO$_3$ is a negative uniaxial crystal, i.e., $n_e < n_0$, the angle θ is negative. For the index ellipsoid in the new

$$\left(\tfrac{1}{n_0^2} - r_{22}E_y\right)x'^2 + \left[\left(\tfrac{1}{n_0^2} + r_{22}E_y\right)\cos^2\theta + \tfrac{\sin^2\theta}{n_e^2} + r_{51}E_y\sin 2\theta\right]y'^2$$
$$+ \left[\left(\tfrac{1}{n_0^2} + r_{22}E_y\right)\sin^2\theta + \tfrac{\cos^2\theta}{n_e^2} - r_{51}E_y\sin 2\theta\right]z'^2 = 1. \tag{5.27}$$

For $\theta \sim \sin\theta$ and $\cos\theta \sim 1$, we obtain

$$\left(\tfrac{1}{n_0^2} - r_{22}E_y\right)x'^2 + \left(\tfrac{1}{n_0^2} + r_{22}E_y + 2r_{51}E_y\theta + \tfrac{\theta^2}{n_e^2}\right)y'^2$$
$$+ \left[\left(\tfrac{1}{n_0^2} + r_{22}E_y\right)\theta^2 - 2r_{51}E_y\theta + \tfrac{1}{n_e^2}\right]z'^2 = 1. \tag{5.28}$$

So we read off for the indices of the main axes

$$\begin{aligned}
\frac{1}{n_{x'}^2} &= \frac{1}{n_0^2} - r_{22}E_y, \\[2mm]
\frac{1}{n_{y'}^2} &= \frac{1}{n_0^2} + r_{22}E_y + 2r_{51}E_y\theta + \frac{\theta^2}{n_0^2}, \\[2mm]
\frac{1}{n_{z'}^2} &= \left(\frac{1}{n_0^2} + r_{22}E_y\right)\theta^2 - 2r_{51}E_y\theta + \frac{1}{n_e^2}.
\end{aligned} \tag{5.29}$$

Since θ is very small, we can neglect the terms proportional to θ

$$\frac{x^2}{n_x^2} + \frac{y^2}{n_y^2} + \frac{z^2}{n_z^2} = 1, \tag{5.30}$$

with

$$\begin{aligned}
n_x &= \frac{n_0}{\sqrt{1 - n_0^2 r_{22} E_y}} = n_0 \left(1 + \frac{1}{2} n_0^2 r_{22} E_y\right), \\
n_y &= \frac{n_0}{\sqrt{1 + n_0^2 r_{22} E_y}} = n_0 \left(1 - \frac{1}{2} n_0^2 r_{22} E_y\right), \\
n_z &= n_{e.}
\end{aligned} \tag{5.31}$$

Again, if a wave propagates along the z-direction with polarization along the x- or y-direction, see Fig. 5.4, then the two polarizations pick up a differential phase shift

$$\Delta \phi = \frac{2\pi L}{\lambda_0} (n_x - n_y) = \frac{2\pi L n_o^3 r_{22} V}{\lambda_0 d} \tag{5.32}$$

and the corresponding half-wave voltage is

$$V_\pi = \frac{\lambda_0 d}{2 L n_0^3 r_{22}}. \tag{5.33}$$

For the values $d = 5$ mm, $L = 10$ mm, $n_o = 2.3$, $r_{22} = 3.4 \cdot 10^{-12}$ m/V at a wavelength of $\lambda_0 = 530$ nm, we observe the half-wave voltage $V_\pi = 1600$ V.

Another possibility to build a modulator from LiNbO$_3$ is given by the fact that a light wave propagates into y-direction and applying the field along the z-axis. The index ellipsoid then reads

$$\left(\frac{1}{n_0^2} + r_{13}E_z\right)x^2 + \left(\frac{1}{n_0^2} + r_{13}E_z\right)y^2 + \left(\frac{1}{n_e^2} + r_{33}E_z\right)z^2 = 1. \qquad (5.34)$$

In this case, the main axes remain

$$\frac{1}{n_0'^2} = \left(\frac{1}{n_0^2} + r_{13}E_z\right), \qquad (5.35)$$

$$\frac{1}{n_e'^2} = \left(\frac{1}{n_e^2} + r_{33}E_z\right).$$

With $r_{13}E_z \ll 1/n_0^2$ and $r_{33}E_z \ll 1/n_e^2$ we obtain the following refractive indices along the main axes

$$n_0' = \frac{n_0}{\sqrt{1 + r_{13}n_0^2 E_z}} = n_0\left(1 - \frac{1}{2}r_{13}n_0^2 E_z\right), \qquad (5.36)$$

$$n_e' = \frac{n_e}{\sqrt{1 + r_{33}n_e^2 E_z}} = n_e\left(1 - \frac{1}{2}r_{33}n_e^2 E_z\right).$$

With these expressions, we obtain for the differential phase shift between ordinary and extraordinary wave

$$\Delta\phi = \frac{2\pi L}{\lambda_0}\left(n'_e - n'_0\right), \qquad (5.37)$$

$$\Delta\phi = \frac{2\pi L}{\lambda_0}\left[n_e - n_0 + \frac{1}{2}\left(r_{33}n_e^3 - r_{13}n_o^3\right)E_z\right]. \qquad (5.38)$$

The half-wave voltage is then

$$V_\pi = \frac{\lambda_0 d}{L\left(r_{33}n_e^3 - r_{13}n_0^3\right)}. \qquad (5.39)$$

With the values $d = 5$ mm, $L = 10$ mm, $r_{33}n_e^3 - r_{13}n_0^3 = 224$ pm/V at a wavelength of $\lambda_0 = 530$ nm, we obtain a half-wave voltage $V_\pi = 1183$ V. Despite the fact that this arrangement shows a lower half-wave voltage than the previous one evaluated by Eq. (5.33), it has a decisive disadvantage. The wave does not propagate along the optical axis, and therefore the crystal acts already as a waveplate even without an applied voltage. The field-independent

Birefringence compensation

phase shift $\Delta\phi_0 = \frac{2\pi L}{\lambda_0}(n_e - n_0)$ depends on temperature, which leads to a temperature-dependent bias. This problem can be mitigated by using two crossed crystals in sequence (o- and e- waves are exchanged in the second crystal, see Fig. 5.6), which cancels the field-independent bias. To avoid cancelation of the field-dependent effect, the field in the second crystal must be poled in reverse.
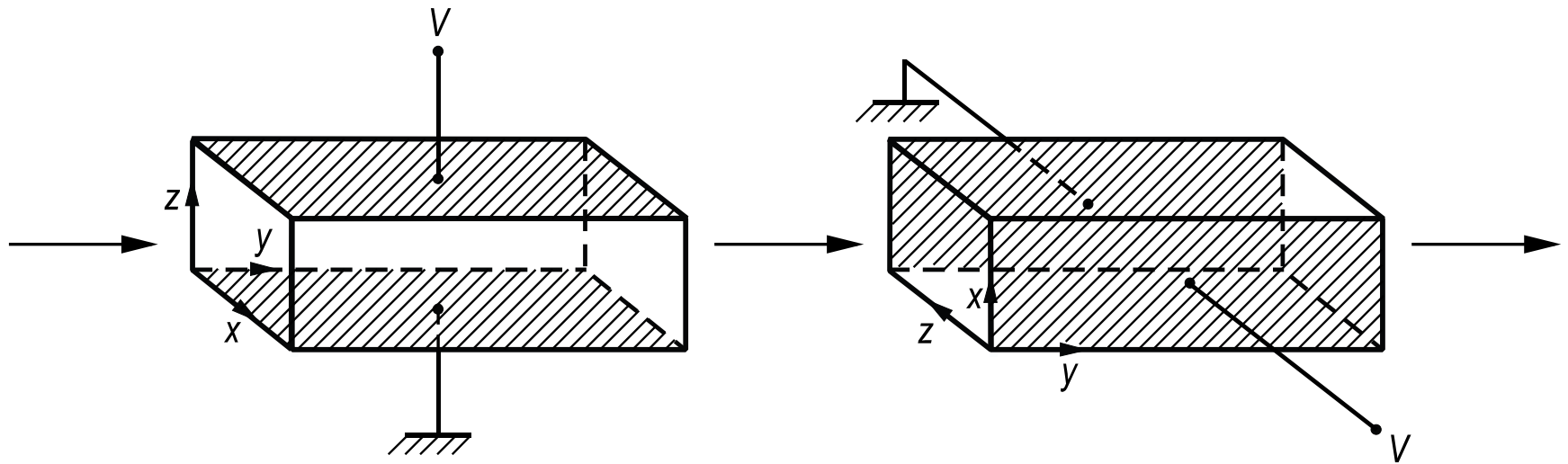

Figure 5.6: Transversal electro-optic modulator using two LiNbO$_3$ crystals rotated by 90° to compensate the field-independent birefringence.

5.2 Electro-optic amplitude modulator

How is phase retardation converted into a amplitude modulation?
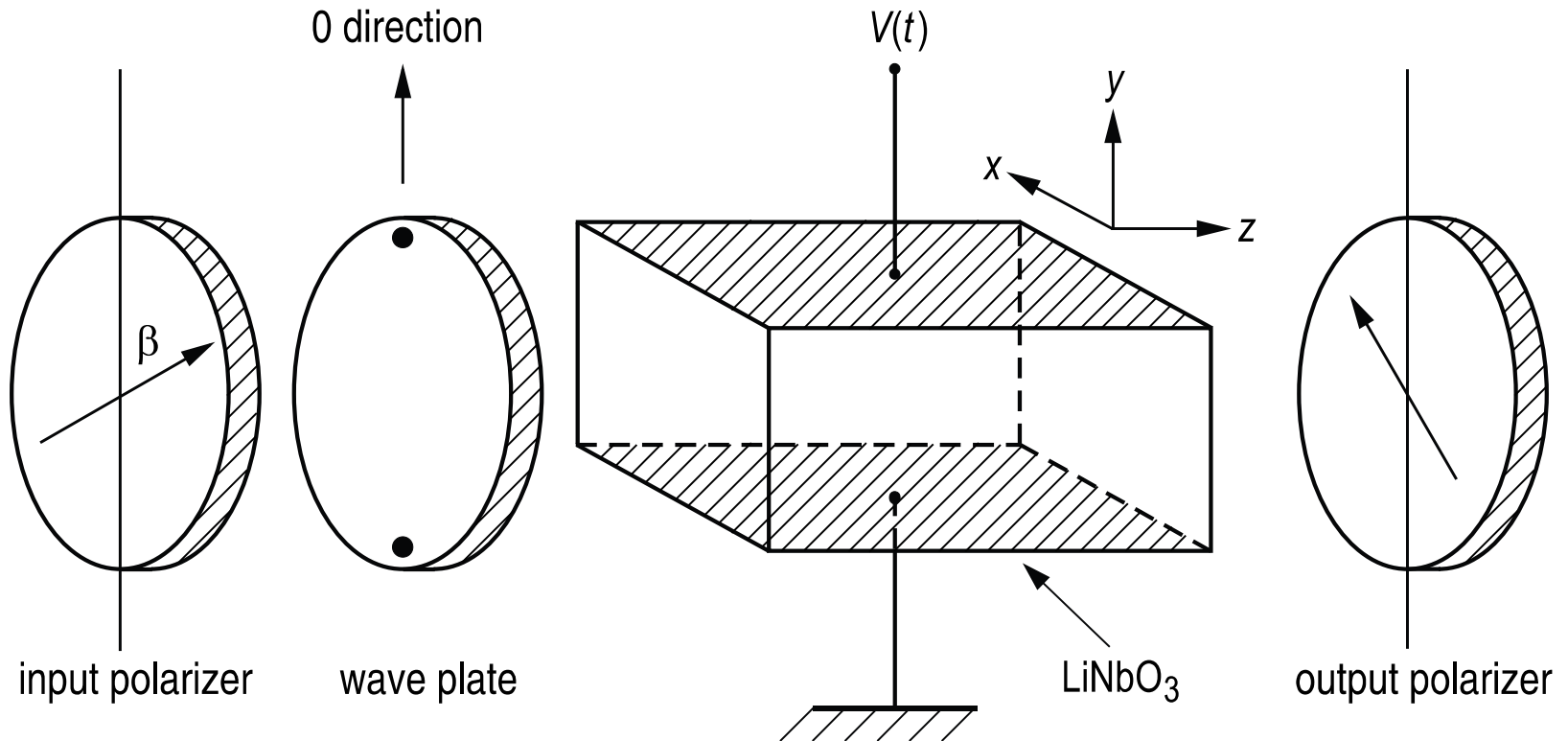

Figure 5.7: Transversal electro-optic amplitude modulator from LiNbO$_3$.

Here, $\Delta\phi_{WP}$ is the phase retardation due to the field-independent birefringence or due to an additional wave plate as shown in Fig. 5.7, and a is a coefficient describing the relationship between field-dependent phase retardation and applied voltage. Usually we use $\beta = 45°$ to achieve 100 % transmission

$$\frac{I_{out}}{I_{in}} = \frac{1}{2}\left\{1 - \cos\left[\Delta\phi_{WP} + aV\left(t\right)\right]\right\} \tag{5.43}$$

$$= \frac{1}{2}\left\{1 - \cos\Delta\phi_{WP}\cos\left[aV\left(t\right)\right] + \sin\Delta\phi_{WP}\sin\left[aV\left(t\right)\right]\right\}.$$

There are various applications for modulators. If the transmission through the modulator should be linearly dependent on the applied voltage, we use a bias $\Delta\phi_{WP} = \pi/2$ and obtain for $aV \ll 1$ (see also Fig. 5.8)

$$\frac{I_{out}}{I_{in}} = \frac{1}{2}\left[1 + aV\left(t\right)\right]. \tag{5.44}$$

For a sinusoidal voltage

$$V\left(t\right) = V_0\sin\omega_m t \tag{5.45}$$

and constant input intensity, we obtain a sinusoidally varying output intensity

$$\frac{I_{out}}{I_{in}} = \frac{1}{2}\left(1 + aV_0\sin\omega_m t\right). \tag{5.46}$$

The constant a can easily be replaced by the half-wave voltage V_π

$$a = \frac{\pi}{V_\pi} = \frac{2\pi L n_0^3 r_{22}}{\lambda_0 d}, \tag{5.47}$$
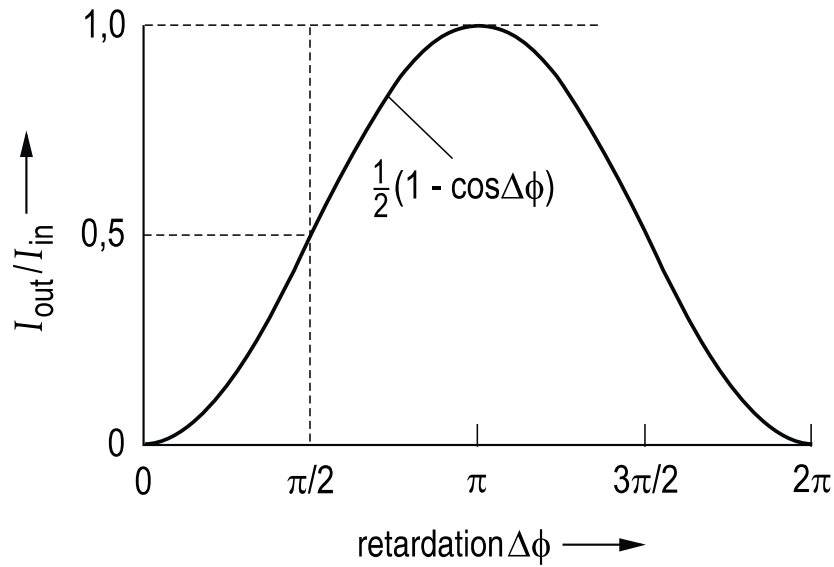
Figure 5.8: Transmission characteristic of the modulator shown in Fig. 5.7 as a function of phase retardation.

where we used Eq. (5.33). With $\Delta\phi_{WP} = 0$, the relationship between output intensity and applied voltage is

$$\frac{I_{out}}{I_{in}} = \frac{1}{2}\left[1 - \cos\left(aV\left(t\right)\right)\right],\tag{5.48}$$

and, for small voltages $aV\left(t\right)$, we obtain a quadratic dependence

$$\frac{I_{out}}{I_{in}} = \frac{1}{4}a^2V^2\left(t\right).\tag{5.49}$$

5.3 Electro-optic phase modulator

If the wave plate and polarizers in Fig. 5.7 are removed and only the ordinary or extraordinary wave is excited, then the electric field after the crystal is

$$E_y^\omega (t) = E_0 \cos \left[\omega t + \phi (t) \right], \tag{5.50}$$

with

$$\phi (t) = \frac{\pi n_0^3 r_{22}}{\lambda_0 d} V (t). \tag{5.51}$$

With a sinusoidal voltage and from Eq. (5.45), we obtain

$$\begin{aligned} E_y^\omega (t) &= E_0 \cos \left(\omega t + m \sin \omega_m t \right) \\ &= E_0 \left[\cos \omega t \cos \left(m \sin \omega_m t \right) - \sin \omega t \sin \left(m \sin \omega_m t \right) \right], \end{aligned} \tag{5.52}$$

with modulation depth m

$$m = \left(\frac{\pi n_0^3 r_{22}}{\lambda_0 d} \right) V_0. \tag{5.53}$$

With the generating functions for the Bessel functions

$$\cos\left(m \sin \omega_m t\right) = J_0\left(m\right) + 2 \sum_{k=1}^{\infty} J_{2k}\left(m\right) \cos\left(2k\omega_m t\right), \qquad (5.54)$$

$$\sin\left(m \sin \omega_m t\right) = 2 \sum_{k=0}^{\infty} J_{2k+1}\left(m\right) \sin\left[\left(2k+1\right)\omega_m t\right], \qquad (5.55)$$

and the addition theorem

$$2 \sin A \sin B = \cos\left(A-B\right) - \cos\left(A+B\right), \qquad (5.56)$$

$$2 \cos A \cos B = \cos\left(A-B\right) + \cos\left(A+B\right), \qquad (5.57)$$

the spectrum of the output field is

$$\begin{aligned} E_y^{\omega}\left(t\right) \quad = \quad & E_0\left[J_0\left(m\right) \cos \omega t \right. \qquad\qquad (5.58) \\ & + J_1\left(m\right) \cos\left(\omega + \omega_m\right) t - J_1\left(m\right) \cos\left(\omega - \omega_m\right) t \\ & + J_2\left(m\right) \cos\left(\omega + 2\omega_m\right) t + J_2\left(m\right) \cos\left(\omega - 2\omega_m\right) t \\ & + J_3\left(m\right) \cos\left(\omega + 3\omega_m\right) t - J_3\left(m\right) \cos\left(\omega - 3\omega_m\right) t \\ & \left. + \ldots \right]. \end{aligned}$$

The spectrum consists of sidebands at multiples of the modulation frequency ω_m. An example is shown in Fig. 5.9.
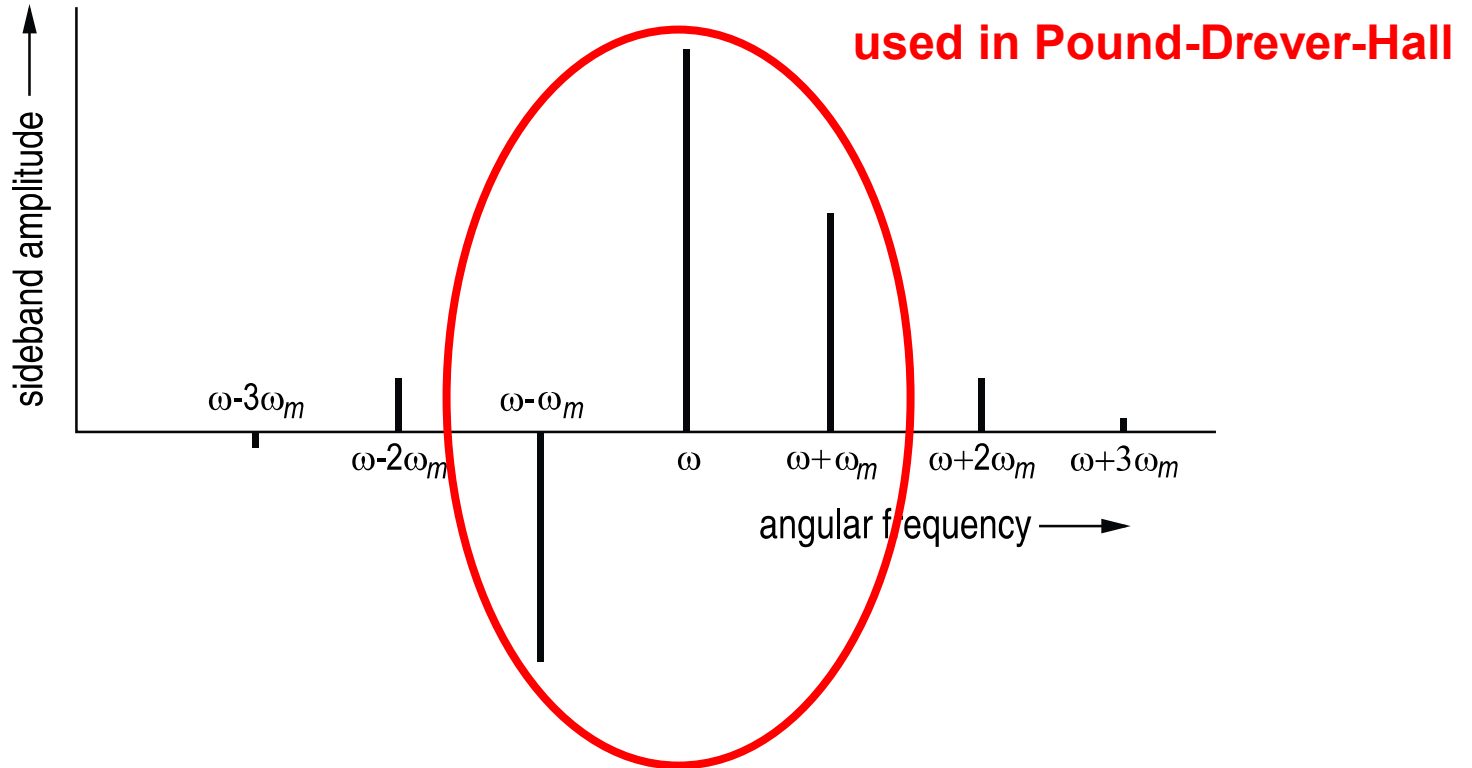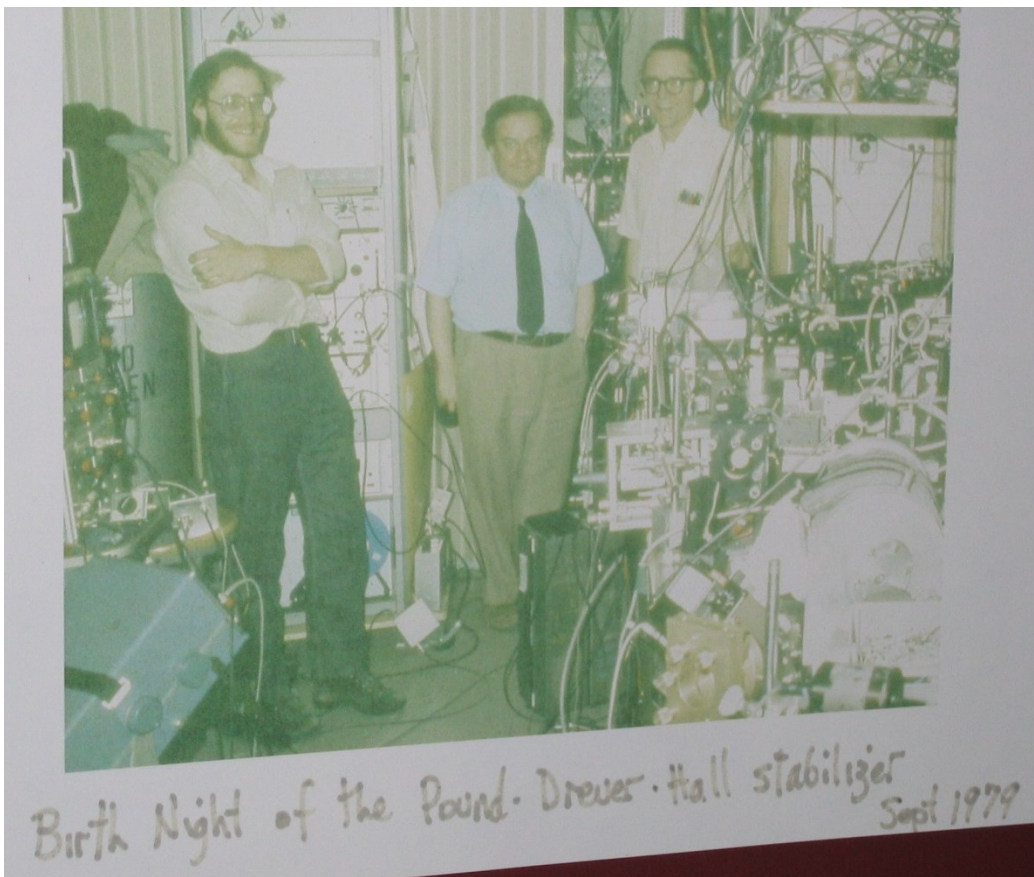

Figure 5.9: Phase-modulated spectrum with a modulation depth of $m = 1$.

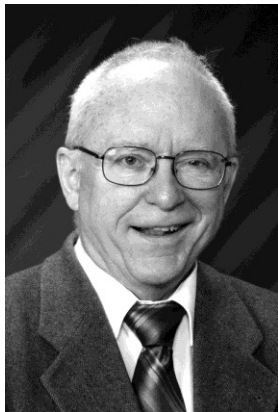Birth Night of the Pound-Drever-Hall stabilizer   Sept 1979

from left to right:
Leo Hollberg, Ronald Drever, John L. Hall

Ronald Drever (1931-2017, co-founder of LIGO)

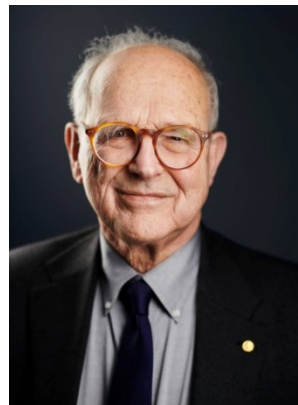Pound-Drever-Hall connected to

2005 Physics Nobel for Hall and Hänsch

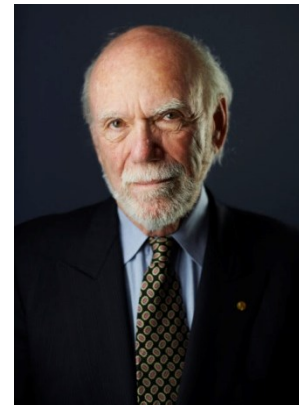2017 Physics Nobel for Weiss, Barish and Thorne

J. L. Hall   T. W. Hänsch   R. Weiss   B. C. Barish   K. S. Thorne

5.4 Microwave modulator

High-speed or microwave signals are typically supplied by strip-lines or coplanar lines, see Eq. 5.10. For efficient modulation, the index modulation must copropagate in phase with the optical signal (group velocity, however, here we neglect dispersion, thus group velocity is equal to phase velocity).
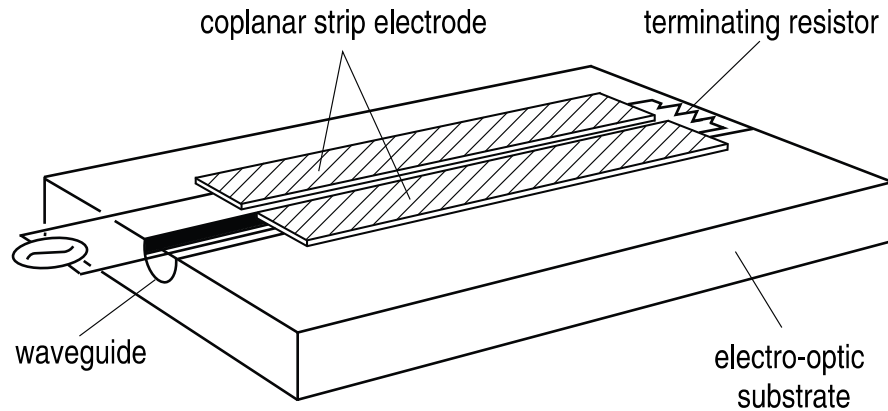

Figure 5.10: Electro-optic traveling wave modulator.

Let's assume the microwave signal

$$V(z,t) = V_0 \cos\left(\omega_m t - \frac{\omega_m n_m}{c_0} z\right), \quad (5.59)$$

with phase velocity

$$c = \frac{c_0}{n_m}. \quad (5.60)$$

If we consider the time slot of the optical wave that enters the crystal at $t = 0$, and copropagate with that time slot in the signal in the waveguide with effective index n, this time slot will experience the applied voltage

$$V(z) = V_0 \cos\left[\frac{\omega_m z}{c_0}(n - n_m)\right] \tag{5.61}$$

at time $t = zn/c_0$. The refractive index change experienced along the waveguide is

$$\Delta n(z) = aV(z), \tag{5.62}$$

and the total integral phase change from input to output is

$$\begin{aligned}
\Delta\phi &= \int_0^\ell \frac{\omega \Delta n(z)}{c_0} dz \\
&= \frac{aV_0\omega}{c_0} \int_0^\ell \cos\left[\frac{\omega_m Z}{c_0}(n - n_m)\right] dz,
\end{aligned} \tag{5.63}$$

or

$$\Delta\phi = \frac{\omega a V_0}{\omega_m \left(n - n_m\right)} \sin\left[\frac{\omega_m \ell}{c_0}\left(n - n_m\right)\right]. \tag{5.64}$$

As shown by Eq. (5.64), the phase modulation is the largest for arg=$\frac{\pi}{2}$, i.e.,

$$\frac{\omega_m \ell \left(n - n_m\right)}{c_0} = \frac{\pi}{2}; \text{ and } \omega_m = \omega_c. \tag{5.65}$$

which determines the optimum length of the modulator. For LiNbO$_3$, with $n_m = 4.2$, $n = 2.146$ and $\ell = 10$ mm, the maximum usable frequency is $\omega_c = 22.9$ GHz. The electric field acts on the waveguide as shown in Fig. 5.11. The waveguide can be fabricated, for example, by indiffusion of titanium. A buffer layer of Al$_2$O$_3$ or SiO$_2$ protects the optical field to interact with the metal electrodes to avoid losses. Typical data for a modulator are: waveguide width 7 μm, thickness of the buffer layer 260 nm, and thickness of the Cr/Au-electrodes is 3 μm. The index difference between core and cladding is about 0.01-0.02. Typical waveguide losses are 1 dB/cm at $\lambda = 633$ nm or 0.3 dB/cm for 1320 nm. The electro-optic tensor for LiNbO$_3$ is

$$\mathbf{r} = \begin{pmatrix} 0 & -3.4 & 8.6 \\ 0 & 3.4 & 8.6 \\ 0 & 0 & 30.8 \\ 0 & 28 & 0 \\ 28 & 0 & 0 \\ -3.4 & 0 & 0 \end{pmatrix} \times 10^{-13} \text{mV}^{-1}. \tag{5.66}$$
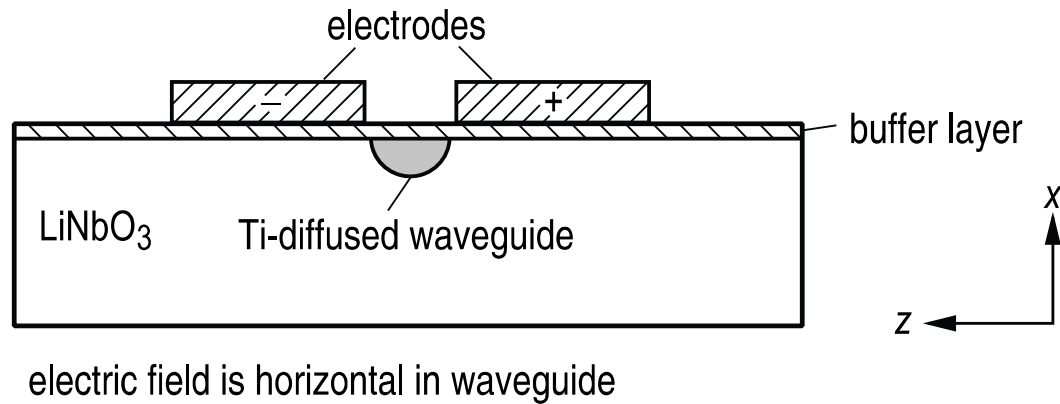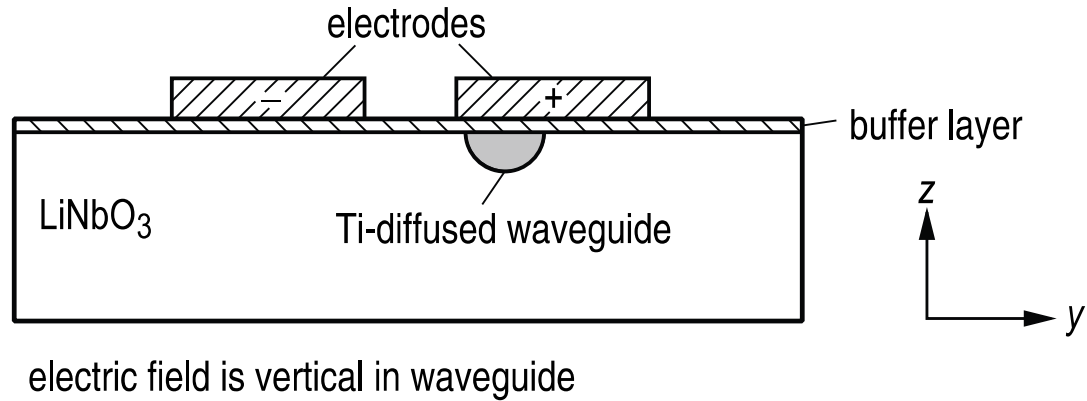
electrodes

−   +

buffer layer

LiNbO$_3$ Ti-diffused waveguide

z

y

electric field is vertical in waveguide

electrodes

−   +

buffer layer

LiNbO$_3$ Ti-diffused waveguide

x

z

electric field is horizontal in waveguide

Figure 5.11: Geometry of a LiNbO$_3$ waveguide modulator: a) z-cut, TM mode b) x-cut, TE mode.